

Enhancement and reentrance of spin triplet superconductivity in UTe_2 under pressureSheng Ran ^{1,2,3} Hyunsoo Kim,¹ I-Lin Liu ^{1,2,3} Shanta R. Saha,^{1,2} Ian Hayes,¹ Tristin Metz,¹ Yun Suk Eo,¹ Johnpierre Paglione,^{1,2} and Nicholas P. Butch^{1,2}¹*Quantum Materials Center, Department of Physics, University of Maryland, College Park, Maryland 20742, USA*²*NIST Center for Neutron Research, National Institute of Standards and Technology, Gaithersburg, Maryland 20899, USA*³*Department of Materials Science and Engineering, University of Maryland, College Park, Maryland 20742, USA*

(Received 29 September 2019; revised manuscript received 16 March 2020; accepted 19 March 2020; published 14 April 2020)

Spin triplet superconductivity in the Kondo lattice UTe_2 appears to be associated with spin fluctuations originating from incipient ferromagnetic order. Here we show clear evidence of twofold enhancement of superconductivity under pressure, which discontinuously transitions to magnetic order, likely of ferromagnetic nature, at higher pressures. The application of a magnetic field tunes the system back across a first-order phase boundary. Straddling this phase boundary, we find another example of reentrant superconductivity in UTe_2 . As the superconductivity and magnetism exist on two opposite sides of the first-order phase boundary, our results indicate other microscopic mechanisms may be playing a role in stabilizing spin triplet superconductivity in addition to spin fluctuations associated with magnetism.

DOI: [10.1103/PhysRevB.101.140503](https://doi.org/10.1103/PhysRevB.101.140503)

While proximity to antiferromagnetism is believed to be a key ingredient for unconventional superconductivity (SC), ferromagnetism (FM) is generally antagonistic and incompatible with superconductivity. In a very few cases [1–3], where FM and SC coexist and are carried by the same electrons, magnetic fluctuations tend to induce triplet pairing, which is a natural candidate for topological SC [4]. Understanding the mechanisms that helps to stabilize triplet SC is therefore important both at the fundamental quantum mechanics level as well as for potential application for quantum computation.

The recently discovered heavy fermion superconductor UTe_2 [5,6], as a paramagnetic end member of the ferromagnetic superconductor series, provides a new platform to study the interaction between FM and triplet SC. The triplet pairing in UTe_2 is clearly manifested by striking experimental results: a remarkably large and anisotropic upper critical field; temperature-independent nuclear magnetic resonance (NMR) Knight shift [5,7]; two independent reentrant superconducting phases existing in extremely high magnetic fields [8,9]; and point node gap structure demonstrated by thermal conductivity, penetration depth [10], and specific-heat measurements [5,6]. Scanning tunneling microscopy (STM) measurements further reveal signatures of chiral in-gap states predicted to exist on the boundary of a topological superconductor [11].

Unlike the ferromagnetic superconductors that share some common features with UTe_2 [1–3], UTe_2 does not order magnetically prior to the onset of SC [5,12]. Instead, scaling analysis shows that it is close to FM quantum criticality [5]. Strong, nearly critical fluctuations have been revealed by NMR [13] and muon spin relaxation measurements [14]. Therefore, a quantum phase transition into a magnetic phase

is likely to be revealed by tuning the system with pressure.

Here we report twofold enhancement of spin triplet SC in UTe_2 [5] under pressure. This occurs as an energy scale is continuously suppressed, the origin of which may be related to Kondo physics. At higher pressures, magnetic order emerges with a first-order phase transition. This phase boundary can be crossed again by applying a magnetic field which increases hybridization, and SC reenters. This shows that multiple microscopic mechanisms conspire to strengthen SC.

Single crystals of UTe_2 were synthesized by the chemical vapor transport method using iodine as the transport agent. A nonmagnetic piston-cylinder pressure cell was used for electrical transport measurements under pressure up to 1.7 GPa, with Daphne oil 7373 as the pressure medium. Transport measurements were performed in a Quantum Design physical property measurement system, and in an Oxford ^3He system [15]. The current was applied in the (011) plane. The magnetic field is about 30° away from the a axis towards the bc plane, which was calibrated using the anisotropic critical field value of superconducting transition. Magnetic susceptibility measurements under hydrostatic pressure were performed in a Quantum Design magnetic property measurement system using a BeCu piston-cylinder clamp cell with Daphne oil as pressure medium. In both cases, pressure produced on the single-crystal sample at low temperatures was calibrated by measuring the superconducting transition temperature of lead placed in the cell. The known pressure dependencies of the superconducting transition temperature of Pb [16] were used for this purpose.

Figure 1(a) summarizes the resistivity data as a function of both temperature and pressure in zero magnetic field. Below 1.31 GPa, the transition temperature of SC, T_c , forms a clear

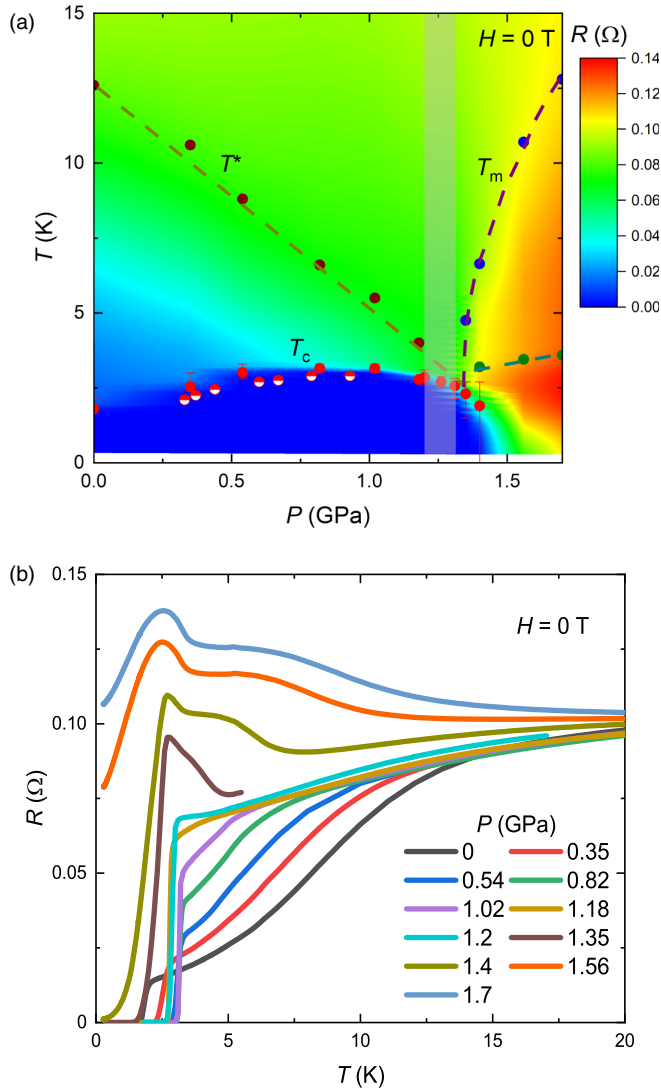


FIG. 1. Phase diagram of UTe_2 under pressure in zero magnetic field. (a) Color contour plot of the resistivity data as a function of both temperature and pressures in zero magnetic field, and the resulting phase diagram. Solid red dots represent the T_c of superconductivity determined from resistance measurements. Error bars are defined by the onset and offset of superconducting transition. The half open red dots represent the T_c of superconductivity determined from magnetization measurements. Brown dots represent the kinks in the $R(T)$ data in the low-pressure range. Blue and green dots represent the local minimums in the $R(T)$ data in the high-pressure range. The gray region indicates the critical pressure region of finite width. Note that for 1.4 GPa, the resistance shows a dramatic drop without reaching zero. Superconductivity reenters in the magnetic field. (b) The temperature dependence of resistivity data in zero magnetic field for selected pressure values. The low-temperature resistivity exhibits a clear evolution in slope, from positive to negative, as pressure increases.

dome feature under pressure peaked at 1 GPa, where T_c is doubled, compared to the ambient pressure value, reaching 3.2 K. The bulk nature of the SC is confirmed by magnetization data under pressure up to 0.93 GPa, measured down to 1.8 K [17].

The enhancement of T_c is accompanied by a systematic change in the low-temperature normal-state resistance value [Fig. 1(b)]. At ambient pressure, the resistivity in the normal state continuously decreases and shows a slope change. The temperature of this slope change T^* is very sensitive to the current direction. In this study, the current flows in the (011) plane, and the slope change appears at 13 K at ambient pressure. As pressure increases, T^* is monotonically suppressed from 13 K to about 5 K for 1.02 GPa, and at higher pressures the signature is no longer visible. Suppression with pressure of scattering associated with T^* is also evident in $R(H)$ curves, as shown in the Supplemental Material [17]. For temperatures above T^* , resistivity scales with a temperature-dependent effective field fairly well, indicating magnetoresistance is governed by one energy scale, and it starts to deviate at low temperatures. The evolution of the temperature range for scaling is consistent with the suppression of T^* , e.g., for 0.45 GPa, the scaling is achieved above 10 K, while for 1.18 GPa, the scaling works from temperatures above T_c .

It is possible that the energy scale suppressed under pressure is associated with the Kondo coherence. At ambient pressure, the resistivity in the normal state shows standard behaviors of Kondo lattice materials: at high temperatures, $R(T)$ slightly increases upon decrease of temperature due to the single-ion Kondo hybridization with the conduction band, while at low temperatures, $R(T)$ suddenly drops due to the formation of Kondo coherence. The formation of Kondo coherence is also evidenced in the magnetization which decreases along the b axis and becomes temperature independent [5], as well as the recent STM measurements showing a clear resonance feature interpreted in terms of a Kondo lattice peak [11]. However, as T^* is very sensitive to the current direction, the slope change of the resistance is likely a result of a combination of Kondo and other scattering process, e.g., scattering from photon and magnetic fluctuations, and therefore T^* may not reflect the exact Kondo coherence temperature. Other measurements under pressure, such as magnetization, will help to better resolve the nature of T^* .

As the pressure further increases, both the normal-state and superconducting properties change dramatically. The normal-state resistivity increases upon cooling with two successive local minima indicating phase transitions. The temperature of the lower temperature minimum T_p does not change much with pressure or magnetic field [Fig. 2(b)]. The temperature of local minimum at higher temperature T_m increases with pressure, and is highly sensitive to the magnetic field, e.g., suppressed from 7 K to 4 K by 6 T, and disappears in higher magnetic field for 1.4 GPa, indicating its magnetic nature [Fig. 2(b)]. Neither T_p nor T_m appear to track to zero temperature. Extrapolations of the pressure dependence of T^* , T_m , T_p , and T_c meet in the critical pressure region, suggesting that a first-order transition occurs when these phenomena have a common finite energy scale.

In an interesting twist, magnetism is suppressed by applied magnetic field, resistivity decreases, and SC is induced, yielding another example of reentrant SC in UTe_2 . This is most apparent at 1.4 GPa. At this pressure, although there is a large drop in the resistivity at low temperatures, a zero resistance state is not achieved (Fig. 2). This is a signature of

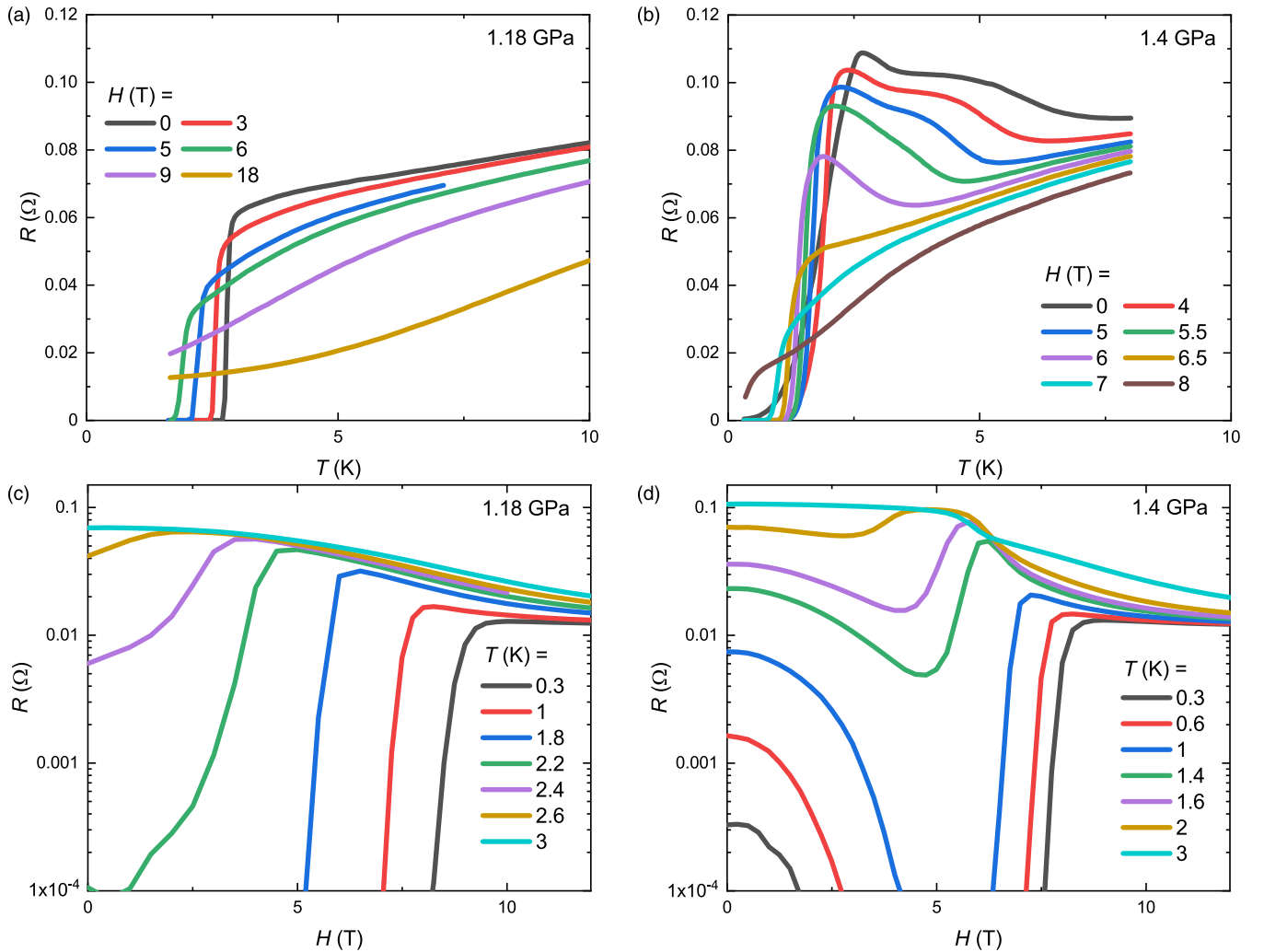


FIG. 2. Magnetic field as a tuning parameter. (a),(b) Resistance data as a function of temperature for different magnetic fields, for 1.18 and 1.4 GPa. Negative normal-state magnetoresistance and sharp upper critical fields are evident. (c),(d) Resistance data as a function of magnetic field for different temperatures, for 1.18 and 1.4 GPa. Reentrant SC is readily apparent in the low-temperature magnetoresistance.

partial volume SC, which is stabilized by local strains on the high-pressure side of the first-order phase transition. As the magnetic field is increased, the resistivity finally drops to zero. This reentrant SC is stable between fields of 2 and 8 T, and appears to be related to the sharply suppressed magnetic order. Similar reentrance of SC in the magnetic field is also observed for 1.35 GPa, but only at 1.6 K, not the zero-temperature limit.

In the region of partial volume SC [gray region in Fig. 3(a)], we observe fairly large hysteresis in the magnetic field dependence of R data [Fig. 3(c)]. Below 2 K, the resistivity increases quickly upon up-sweep in the very low field range, leading to a larger value than that upon down-sweep. Above the gray region, the hysteresis disappears. Such hysteresis is typically associated with FM domain motion, indicating the magnetism under high pressure is FM. On the other hand, the hysteresis observed here is only seen at temperatures below the sudden drop of resistivity,

suggesting the role of an additional mechanism. Due to the first-order phase transition separating SC and FM as a function of pressure, both phases can coexist heterogeneously. The relative volume fractions are different upon up- and down-sweep of magnetic field, leading to the hysteresis. The first-order nature of T_m is more obvious when it is suppressed to lower temperatures by applied field. As shown in Fig. 3(b), in 6 T, $R(T)$ also shows well-defined hysteresis in temperature. Similar hysteresis is observed at lower pressure in zero field [17]. As FM quantum phase transitions are discontinuous in clean metallic systems [18] yet can still act as a source of strong order parameter fluctuations [19], this critical pressure-field region emerges as a likely source of the strong spin fluctuations observed in UTe_2 at ambient pressure.

Two other reentrant superconducting phases have been already observed in UTe_2 under high magnetic field [8,9], at ambient pressure, which are likely induced by ferromagnetic

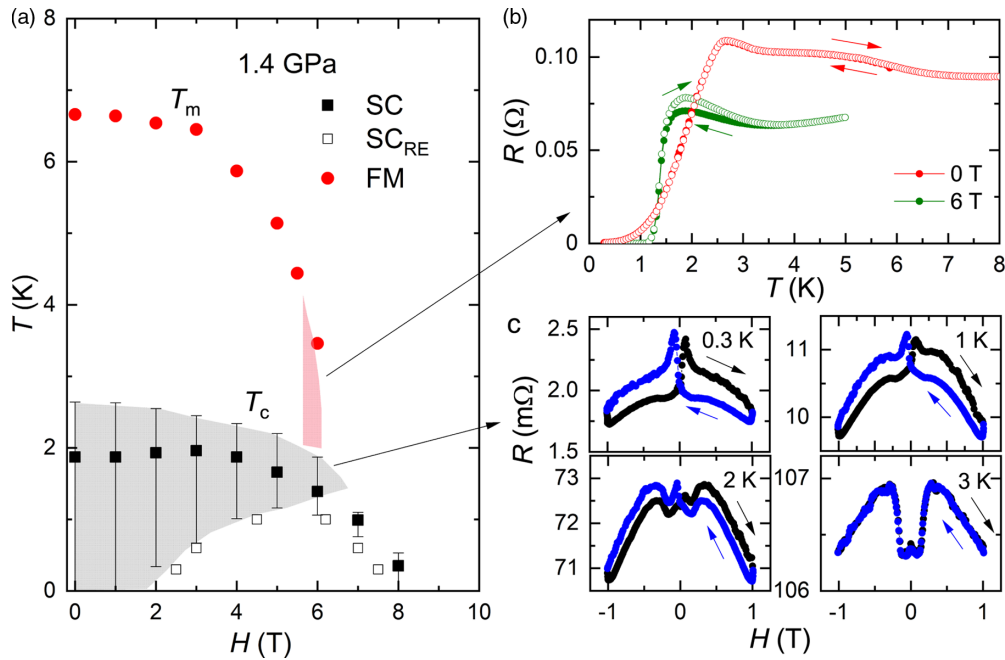


FIG. 3. Hysteresis in temperature and magnetic field for 1.4 GPa. (a) Magnetic and superconducting phase boundaries at 1.4 GPa. In the pink region hysteresis is observed in the temperature-dependent resistance data. In the gray region, superconductivity coexists with magnetism, and hysteresis is observed in the field-dependent resistance data. Error bars of T_c are defined by the onset and offset of superconducting transition. (b) Resistance data as a function of temperature for $H = 0$ and 6 T, showing clear hysteresis in temperature when the magnetic phase is suppressed to low enough temperature. (c) Resistance data as a function of magnetic field from -1 to 1 T for 0.3, 1, 2, and 3 K, showing hysteresis in magnetic field in the region where superconductivity coexists with magnetism.

fluctuations and decreased dimensionality. The reentrant superconducting phase observed under pressure is quite different. First, the magnetic field scale is much smaller here. In addition, in this case reentrant SC exists on both sides of the magnetic phase boundary, while in the case of the field-induced SC at ambient pressure, SC only exists in the field polarized state [8]. These differences indicate the reentrance of SC is probably due to a different mechanism. The domelike feature and the suppression of multiple energy scales in the vicinity of optimal SC indicate that SC is closely related with fluctuations from the competition of these energy scales.

The pressure dependence of UTe_2 is qualitatively different from that of the ferromagnetic superconductors [20], in which case SC coexists with FM. For UGe_2 and URhGe , SC exclusively exists inside the FM region, while for UCoGe , SC exists on both sides of the FM boundary [20]. In all these cases, FM fluctuations are believed to be responsible for the triplet pairing [21]. In general, the role of electronic instabilities in the ferromagnetic superconductors remains an open question; even in the case of UGe_2 , where changes in magnetic order coincide with apparent Fermi surface changes, SC is not a ground state on the paramagnetic side [20]. However, in pressure-tuned UTe_2 , SC and magnetism exist on two opposite sides of the phase boundary (Fig. 4). This

insight may help to better understand the FM superconductors and further reveals a new paradigm for enhancing spin triplet SC.

Note added. Recently, Braithwaite *et al.* independently reported specific-heat and transport measurements on UTe_2 under pressure [22]. Their observation of a pressure-enhanced superconducting transition temperature and emergence of a higher pressure magnetic phase is consistent with our results. They observe multiple superconducting phases under pressure in specific-heat measurements, which cannot be observed in transport measurements.

We acknowledge S. L. Bud'ko and P. C. Canfield for providing the pressure medium. S.R. is grateful for inspiring discussions with Y. F. Yang and Y. Wang. We acknowledge W. T. Fuhrman for assistance during sample synthesis. We also acknowledge H. Hodovanets for helpful assistance during our experiments. The Research at the University of Maryland was supported by the National Institute of Standards and Technology (NIST), the U.S. National Science Foundation (NSF) Division of Materials Research Award No. DMR-1610349, the U.S. Department of Energy (DOE) Award No. DE-SC-0019154 (experimental investigations), and the Gordon and Betty Moore Foundation's EPiQS Initiative through Grant No. GBMF4419 (materials synthesis).

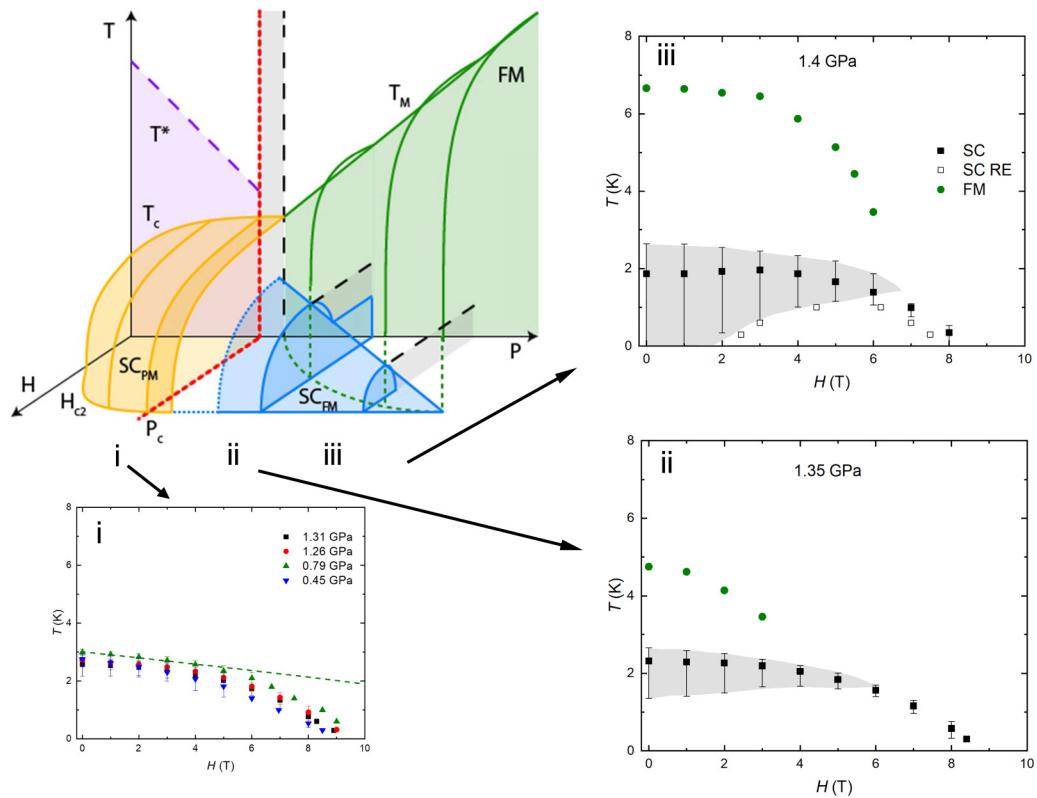


FIG. 4. Schematic phase diagram of UTe_2 , emphasizing the opposing roles of pressure P and magnetic field H as tuning parameters. For clarity, only one of the phase transitions in the high-pressure region is plotted. In the low-pressure region, paramagnetic superconductivity SC_{PM} (in yellow) exists below T^* . On the high-pressure side of the critical pressure P_c , magnetic order (green) is suppressed by field, and reentrant superconductivity SC_{FM} is observed at low temperature (blue). Coexistence of magnetism and SC is observed at these pressures. Constant pressure slices are shown for low pressure (i), 1.35 GPa (ii), and 1.4 GPa (iii). In (i), the T and H limits of superconductivity are rather pressure insensitive. In (ii) and (iii), the magnetism/SC coexistence regions are marked in gray, and the relationship between optimal SC and suppression of magnetism are clearly seen. Error bars of T_c are defined by the onset and offset of superconducting transition.

- [1] S. S. Saxena, P. Agarwal, K. Ahilan, F. M. Grosche, R. K. W. Haselwimmer, M. J. Steiner, E. Pugh, I. R. Walker, S. R. Julian, P. Monthoux, G. G. Lonzarich, A. Huxley, I. Sheikin, D. Braithwaite, and J. Flouquet, *Nature (London)* **406**, 587 (2000).
- [2] D. Aoki, A. Huxley, E. Ressouche, D. Braithwaite, J. Flouquet, J.-P. Brison, E. Lhotel, and C. Paulsen, *Nature (London)* **413**, 613 (2001).
- [3] N. T. Huy, A. Gasparini, D. E. de Nijs, Y. Huang, J. C. P. Klaasse, T. Gortenmulder, A. de Visser, A. Hamann, T. Görlach, and H. v. Löhneysen, *Phys. Rev. Lett.* **99**, 067006 (2007).
- [4] M. Sato and Y. Ando, *Rep. Prog. Phys.* **80**, 076501 (2017).
- [5] S. Ran, C. Eckberg, Q.-P. Ding, Y. Furukawa, T. Metz, S. R. Saha, I.-L. Liu, M. Zic, H. Kim, J. Paglione, and N. P. Butch, *Science* **365**, 684 (2019).
- [6] D. Aoki, A. Nakamura, F. Honda, D. Li, Y. Homma, Y. Shimizu, Y. J. Sato, G. Knebel, J.-P. Brison, A. Pourret, D. Braithwaite, G. Lapertot, Q. Niu, M. Vališka, H. Harima, and J. Flouquet, *J. Phys. Soc. Jpn.* **88**, 043702 (2019).
- [7] G. Nakamine, S. Kitagawa, K. Ishida, Y. Tokunaga, H. Sakai, S. Kambe, A. Nakamura, Y. Shimizu, Y. Homma, D. Li, F. Honda, and D. Aoki, *J. Phys. Soc. Jpn.* **88**, 113703 (2020).
- [8] S. Ran, I.-L. Liu, Y. S. Eo, D. J. Campbell, P. Neves, W. T. Fuhrman, S. R. Saha, C. Eckberg, H. Kim, J. Paglione, D. Graf, J. Singleton, and N. P. Butch, *Nat. Phys.* **15**, 1250 (2019).
- [9] G. Knebel, W. Knafo, A. Pourret, Q. Niu, M. Vališka, D. Braithwaite, G. Lapertot, M. Nardone, A. Zitouni, S. Mishra, I. Sheikin, G. Seyfarth, J.-P. Brison, D. Aoki, and J. Flouquet, *J. Phys. Soc. Jpn.* **88**, 063707 (2019).
- [10] T. Metz, S. Bae, S. Ran, I.-L. Liu, Y. S. Eo, W. T. Fuhrman, D. F. Agterberg, S. Anlage, N. P. Butch, and J. Paglione, *Phys. Rev. B* **100**, 220504(R) (2019).
- [11] L. Jiao, Z. Wang, S. Ran, J. O. Rodriguez, M. Sigrist, Z. Wang, N. Butch, and V. Madhavan, *Nature* **579**, 523 (2020).
- [12] V. Hutano, H. Deng, S. Ran, W. T. Fuhrman, H. Thoma, and N. P. Butch, *Acta Cryst. B* **76**, 137 (2020).
- [13] Y. Tokunaga, H. Sakai, S. Kambe, T. Hattori, N. Higa, G. Nakamine, S. Kitagawa, K. Ishida, A. Nakamura, Y. Shimizu, Y. Homma, D. Li, F. Honda, and D. Aoki, *J. Phys. Soc. Jpn.* **88**, 073701 (2019).
- [14] S. Sundar, S. Gheidi, K. Akintola, A. M. Cote, S. R. Dunsiger, S. Ran, N. P. Butch, S. R. Saha, J. Paglione, and J. E. Sonier, *Phys. Rev. B* **100**, 140502(R) (2019).
- [15] Identification of commercial equipment does not imply recommendation or endorsement by NIST.
- [16] T. F. Smith and C. W. Chu, *Phys. Rev.* **159**, 353 (1967).
- [17] See Supplemental Material at <http://link.aps.org/supplemental/10.1103/PhysRevB.101.140503> for more data.

- [18] M. Brando, D. Belitz, F. M. Grosche, and T. R. Kirkpatrick, *Rev. Mod. Phys.* **88**, 025006 (2016).
- [19] P. Schmakat, M. Wagner, R. Ritz, A. Bauer, M. Brando, M. Deppe, W. Duncan, C. Duvinage, C. Franz, C. Geibel, F. M. Grosche, M. Hirschberger, K. Hradil, M. Meven, A. Neubauer, M. Schulz, A. Senyshyn, S. Süllow, B. Pedersen, P. Böni, and C. Pfleiderer, *Eur. Phys. J.: Spec. Top.* **224**, 1041 (2015).
- [20] D. Aoki, K. Ishida, and J. Flouquet, *J. Phys. Soc. Jpn.* **88**, 022001 (2019).
- [21] V. P. Mineev, *Phys. Usp.* **60**, 121 (2017).
- [22] D. Braithwaite, M. Vališka, G. Knebel, G. Lapertot, J.-P. Brison, A. Pourret, M. E. Zhitomirsky, J. Flouquet, F. Honda, and D. Aoki, *Commun. Phys.* **2**, 147 (2019).

Supplemental material: Enhancement and reentrance of spin triplet superconductivity in UTe_2

Sheng Ran^{1,2,3}, Hyunsoo Kim¹, I-Lin Liu^{1,2,3}, Shanta Saha^{1,2}, Ian Hayes¹,
Tristin Metz¹, Yun Suk Eo¹, Johnpierre Paglione^{1,2}, Nicholas P. Butch^{1,2}

¹ *Center for Nanophysics and Advanced Materials, Department of Physics,
University of Maryland, College Park, MD 20742, USA*

² *NIST Center for Neutron Research,
National Institute of Standards and Technology, Gaithersburg, MD 20899, USA*

³ *Department of Materials Science and Engineering,
University of Maryland, College Park, MD 20742, USA*

(Dated: February 19, 2020)

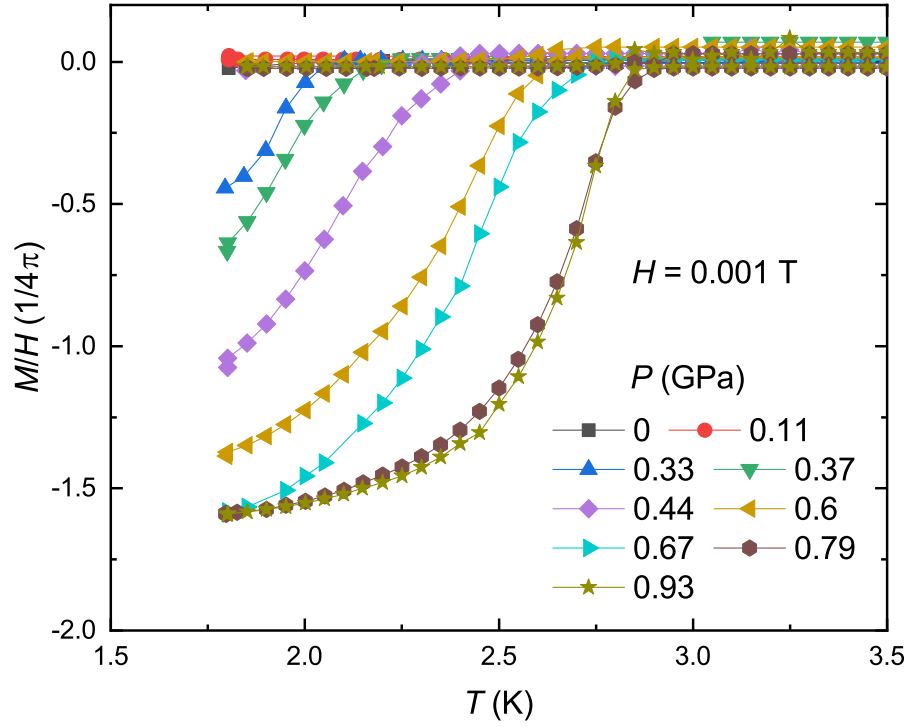


FIG. 1. Magnetization data as a function of temperature for different pressure in magnetic field of 0.001 T, showing bulk nature of superconductivity.

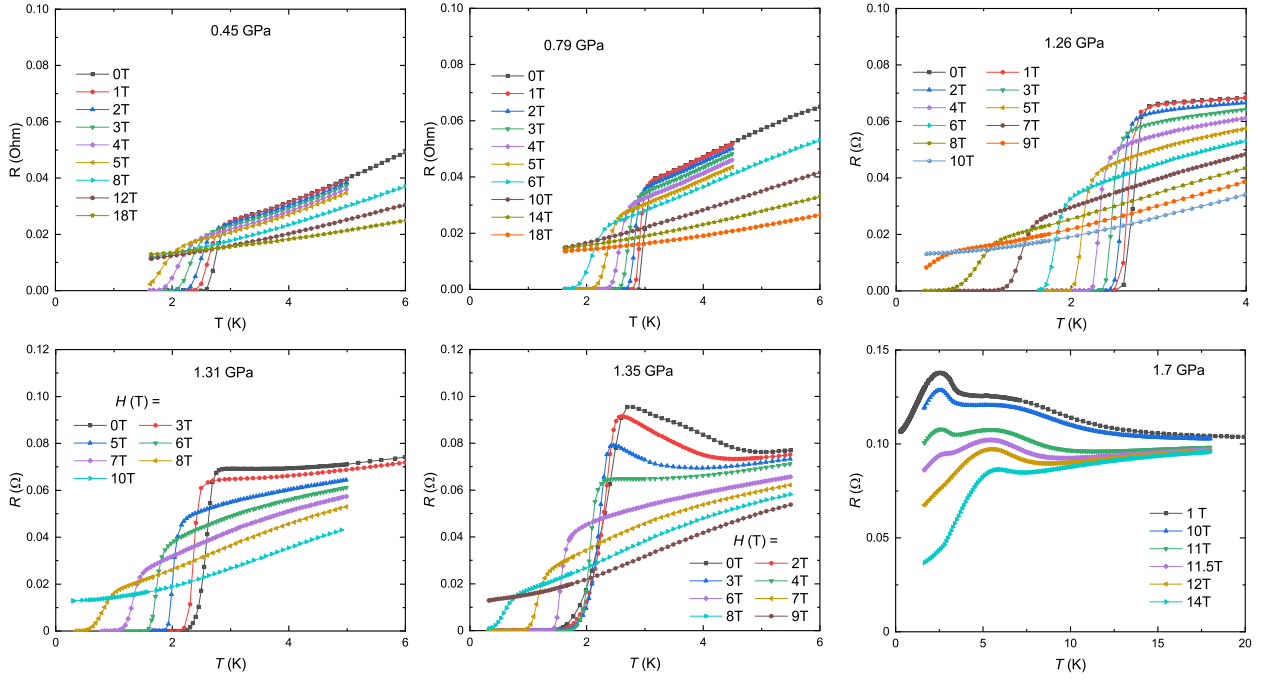


FIG. 2. Resistance data as a function of temperature for different magnetic fields, for additional pressure values, 0.45, 0.79, 1.26, 1.31, 1.35 and 1.7 GPa.

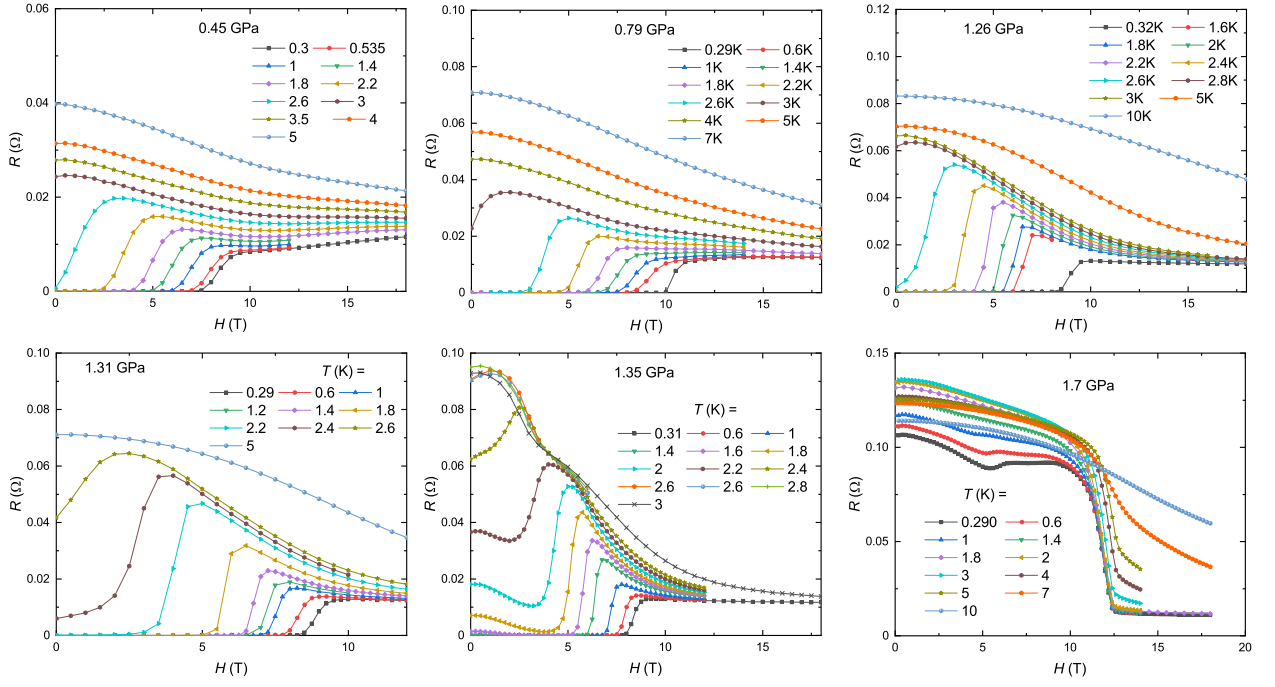


FIG. 3. Resistance data as a function of magnetic field for different temperatures, for additional pressure values, 0.45, 0.79, 1.26, 1.31, 1.35 and 1.7 GPa.

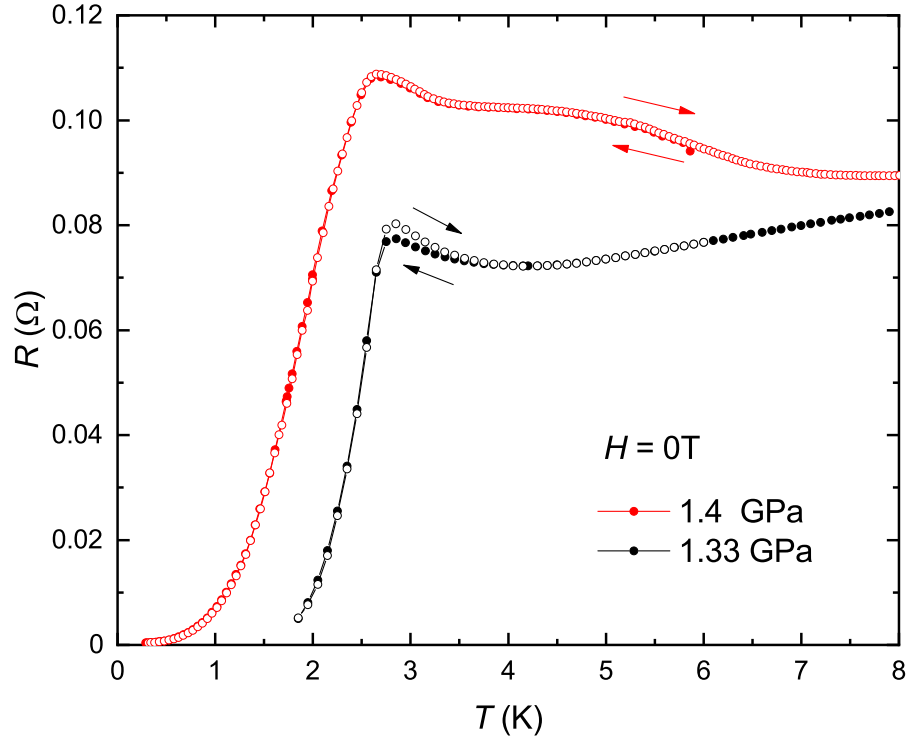


FIG. 4. Resistance data as a function of temperature for $H = 0$, for 1.33 and 1.4 GPa. Weak but well defined hysteresis in temperature is seen for 1.33 GPa.

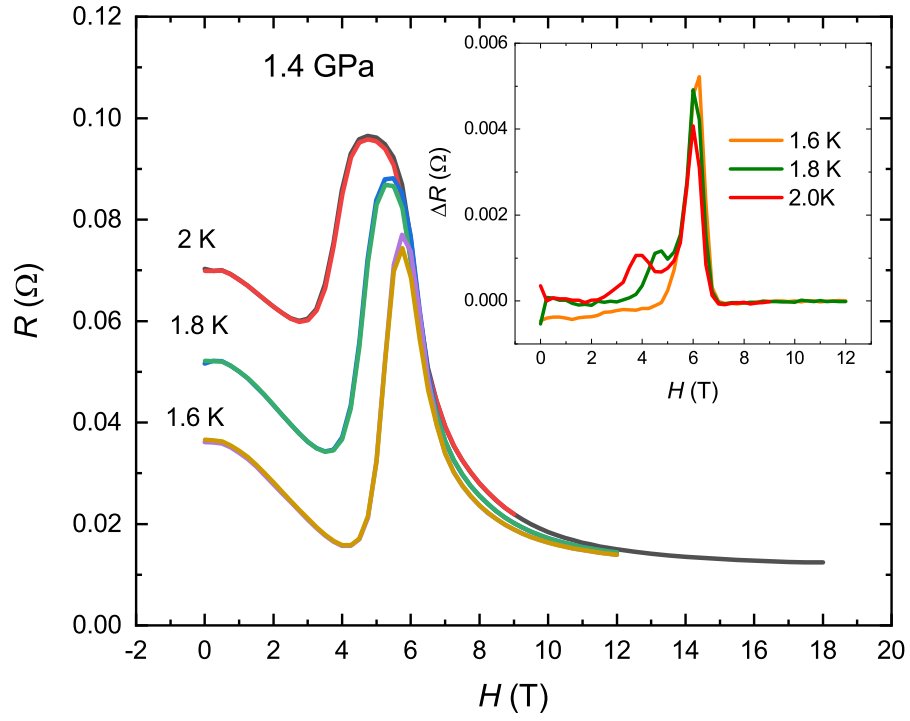


FIG. 5. Resistance data as a function of field for 1.4 GPa, for 1.6, 1.8 and 2 K. Inset: change of resistance value between up and down sweep, showing clear hysteresis.

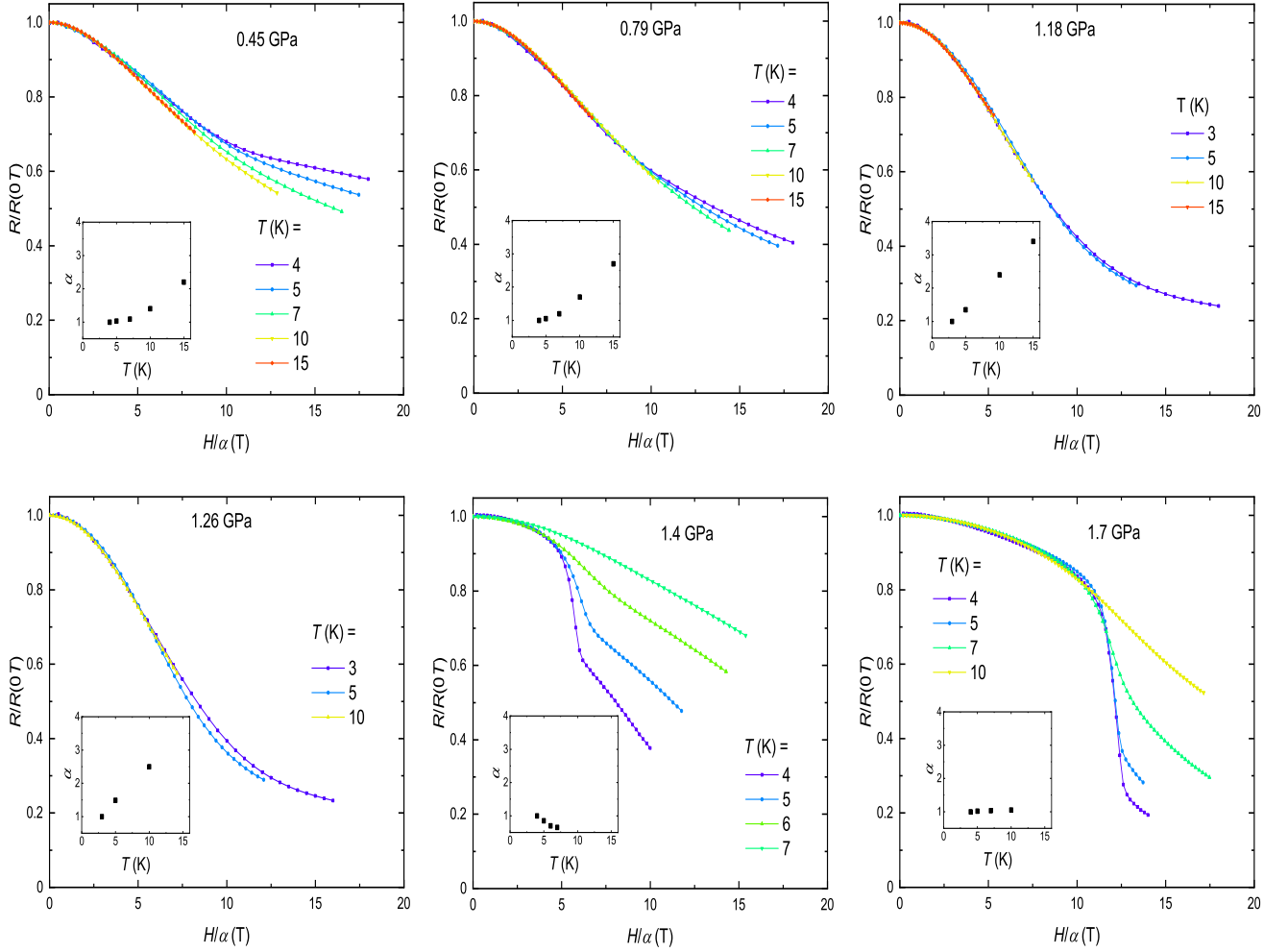


FIG. 6. Resistance data, normalized to the zero field value, as a function of scaled magnetic field H/α for different temperatures, for 0.45, 0.79, 1.18, 1.26, 1.4 and 1.7 GPa. α is an empirical number chosen for the best scaling and is plotted as a function of temperature for each pressure in the inset. In the region where good scaling is achieved, α is roughly linear as a function of temperature, indicating α represents temperature. The minimum temperature for a good scaling decreases with pressure, 10 K for 0.45 GPa, 7 K for 0.79 GPa and 3 K for 1.18 GPa, indicating suppression of an energy scale. Scaling does not work in the high pressure region.

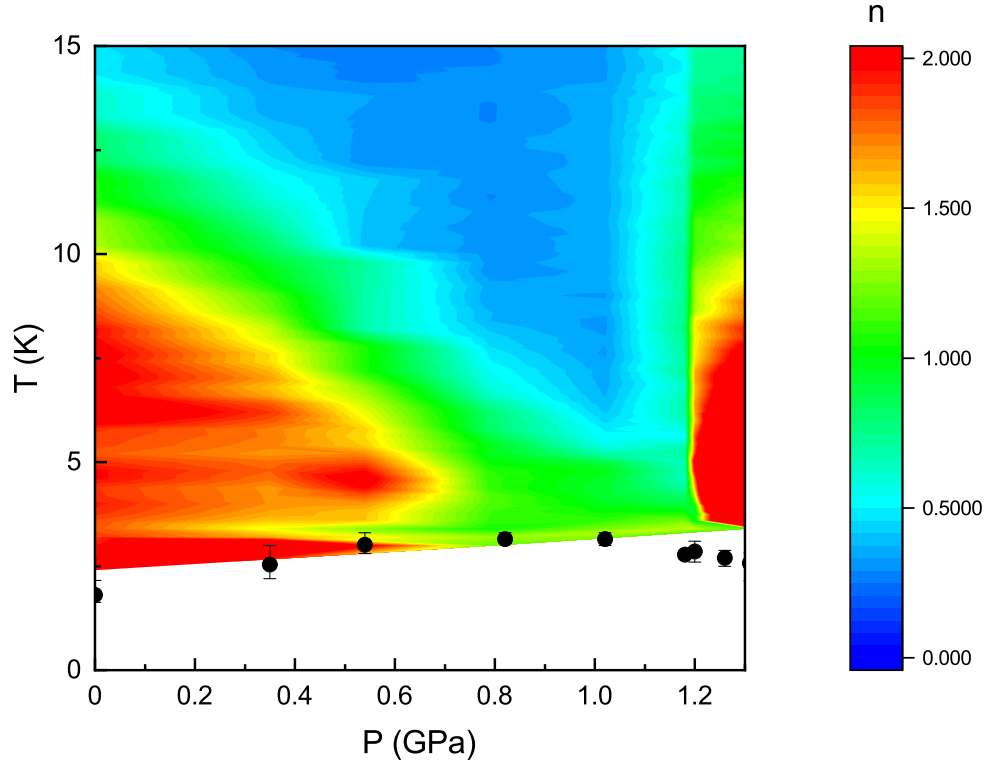


FIG. 7. Power law exponent n , extrapolated from $d(\ln(R(T) - R(T_0)))/d(\ln T)$, as a function of temperature and pressure, in the low pressure region. Non-Fermi liquid behaviour with n between 1 and 1.5 is observed, although the range for power law fit is not large due to the appearance of superconductivity. White region is the superconducting phase, where no power law exponent can be extrapolated from resistance data. Black dots represent T_c of superconductivity determined from resistance measurements. Error bars are defined by the onset and offset of superconducting transition.